Received 4 January 2012
Revised 12 March 2012
15 May 2012
Accepted 25 September 2012

Loss of monotonicity and anomalous scaling behavior in the passive scalar gradient

A DNS study on causes of intermittency

Ivan Langella
DETEC, University of Naples Federico II, Naples, Italy
Carlo Scalo
Department of Mechanical and Material Engineering, Queen's University, Kingston, Canada, and
Giuseppe De Felice and Carlo Meola
DETEC, University of Naples Federico II, Naples, Italy

Abstract

Purpose – The purpose of this paper is to discuss some fundamental aspects regarding the anomalies in the passive scalar field advected by forced homogenous and isotropic turbulence, by inspection of the analytical properties of the governing equations and with the aid of direct numerical simulation (DNS) data.

Design/methodology/approach – Results from a pseudo-spectral DNS of a unitary-Schmidt-number passive scalar advected by a low Reynolds number flow field, $Re_\lambda = 50$ and 70 (based on the Taylor microscale λ) allow for a preliminary assessment of the developed numerical model.

Findings – Manipulation of the governing equations for the scalar field (which are monotonic) reveals that the unboundedness of the scalar gradient magnitude is not ruled out by the mathematical properties of the correspondent conservation equation. Classic intermittency effects in the passive scalar field have been reproduced, such as non-Gaussian behavior of the passive scalar statistics, loss of local isotropy, and multi-fractal scaling of scalar structure functions. Moreover, Taylor and Richardson theories are, surprisingly, not confirmed only in the dissipation range (small-scales anomalies).

Originality/value – The authors suggest that the origin of intermittency (qualitatively pictured here as violent burst in spatial gradient quantities) should be sought in the loss of monotonicity of the evolution equation of the scalar gradient.

Keywords Turbulence, Functional analysis, Numerical methods, Monotonicity, Passive scalar, Intermittency, Isotropic turbulence, Vortex stretching

Paper type Research paper

1. Introduction

Recent findings in the study of a passive scalar transported by a turbulent flow reveal how the fundamental ideas underlying the classical KOC theory (Kolmogorov, 1941; Obukhov, 1949) – self-similarity, small-scale universality and return-to-isotropy – are contradicted by the experimental and numerical evidence (Wahraft, 2000). The evolution of the scalar field, $\theta\theta$, is governed by well-known conservation laws yielding a linear PDE in $\theta\theta$. In spite of the linearity of such equation, when the transporting velocity field is turbulent, scalar iso-surfaces stretch and fold transferring scalar

International Journal of Numerical Methods for Heat & Fluid Flow
Vol. 23 No. 1, 2013
pp. 108-123

0961-5539
DOI 10.1108/09615531311289132

variance down the cascade from large-scales to small scales (Kolmogorov, 1941). During this process, for sufficiently high Reynolds numbers, the turbulent cascade is expected to modulate, in the inertial sub-range, the (non-diffusive) scalar variance transfer in such a way that a self-similar statistical state (linear scaling of structure function exponents) is achieved throughout this range of scales. On the contrary, scalar gradients actually grow with a very irregular pattern, both in space and time, and local discontinuities can arise influencing the passive scalar phenomenology. Also, the nature and type of anomalies displayed may be heavily flow-dependent. The definition of "intermittent" encompasses many of these unexpected features of turbulent flows, and, specifically, of the scalar field which is the focus of this paper.

Intermittency in a turbulent flow is often classified as external or internal. External intermittency refers to the extremely irregular appearance and disappearance of turbulent patches, for example, in the turbulent-non-turbulent interface of a jet or a wake, pockets of irrotational fluid are entrained by the turbulent eddies close to the interface (Pope, 2000); on the other hand, internal intermittency (which is composed by dissipation-range intermittency and inertial-range intermittency) refers to the very irregular behavior of the dissipation field (or other quantities) present within a fully developed turbulent flow that is responsible for the lack of self-similarity in the turbulent small-scale structure (Frisch, 1995). Its existence poses serious challenges to the modeling of the small-scale structure of the velocity and, in particular, of the scalar field. The review by Wahraft (2000) is almost entirely centered on such issues, which have become a widespread "obsession" for all the following work in the field. In this paper we will focus on internal intermittency phenomena.

Violent and intermittent bursts in turbulent activity, present at all scales in a fully developed flow, are associated with corresponding peaks in dissipation rates. Meneveau and Sreenivasan (1990) explained the observation of a universal fractal dimension of the rate of dissipation by taking into account the influence of local fluctuation at the smallest scales. Sreenivasan (1991) found that diffusive effects are not negligible in the inertial sub-range and that universal, non-diffusive mechanisms of scalar variance transfer are affected by the direct interaction between large and smaller eddies leading to well defined structures, such as ramps. Kraichnan (1994) has shown that even when the velocity field is strictly Gaussian (non-intermittent and statistically self-similar), the transported passive scalar field exhibits several anomalies including loss of isotropy at the smallest scales and inertial-range intermittency. The loss of local isotropy is testified by the presence of quasi-unitary scalar derivative skewness, ramp-cliff structures in the concentration or temperature time series, large fronts separating sharply "hot" and "cold" regions and sub-linear scaling of the high-order structure functions exponents (Holzer and Siggia, 1994; Antonia *et al.*, 1986). Intermittency effects can be taken into account under certain ranges by using correction factors which modify the Kolmogorov's proportionality to $n/3$ (where n is the scaling exponent) with a lower value ζ_n, so to satisfy the sub-linear behavior. Intermittency correction factors based on relations among structure functions were adopted by Ruiz-Chavarria *et al.* (1996) in order to show that the scalar dissipation scale is smaller than the velocity dissipation scale at Schmidt numbers close to one and that the scalar has a reduced self-similar range. A physical insight into the matter of an isotropic flow in presence of a uniform scalar mean gradient was provided by Vedula *et al.* (2001), who demonstrated that the scalar gradient is responsible for the scalar dissipation fluctuations, exhibiting a non-linear growth amplified by strain rate fluctuations.

Also, the scalar gradient was found to align preferentially to the local flow structures strongly in high turbulent kinetic energy regions. Correlations between the fluctuating rate of strain and scalar dissipation rate was also investigated by Antonia and Orlandi (2003), however, not addressing the (artificial) effects of the linear forcing. Statistical quantities such as skewness, kurtosis, passive scalar gradients and passive scalar differences probability distribution functions (PDFs) (exhibiting exponential tails at all scales independently of the velocity field), and instantaneous events retain the signature of these events (Mydlarsky and Warhaft, 1998; Shraiman and Siggia, 2000; Chen and Kraichnan, 1998). More recently, Sreenivasan and Shumacher (2010) suggest adopting a Lagrangian approach, consistently with the intrinsic mechanisms of turbulence. Despite the great experimental and numerical effort, the implications on intermittency of more basic mathematical properties of the governing equations might have been overlooked. The conservation equation for the passive scalar is monotonic: the convection-diffusion equation is linear and conservative, therefore, the value of the scalar is bounded by the initial and boundary conditions (Leveque, 2002); the passive scalar value cannot exceed or be lower than the lowest or highest value present initially in the field or at the boundary. From a Lagrangian view point, along every path line, the solution is bounded by the maximum and minimum value at the initial time along that path line. This is not the case for the scalar gradient field, as shown in this work. Given this framework of ideas and results on intermittency, in the following we want to analyze this problem by looking at the mathematical properties of the governing equations for the scalar transport and the scalar gradient first and then by presenting some preliminary numerical results in direct numerical simulation (DNS) of forced homogeneous and isotropic turbulence, that will lead the way to future numerical investigations. Also, an attempt is made at analyzing the numerical results (as well as theoretical results for the governing PDEs) to deduce whether or not the Navier-Stokes equations, in their incompressible form, are a suitable model to study intermittency effects. The possible presence of spatial discontinuities in a turbulent flow is excluded a priori by the incompressible mathematical model, which does not allow for the existence of weak solutions: only smooth solutions can be observed, posing unnecessary limitations to the physics being investigated.

2. Problem formulation

Both our analytical and numerical investigations are based on the fundamental governing equations for an incompressible velocity field:

$$\frac{\partial u_j}{\partial x_j} = 0 \tag{1}$$

$$\frac{\partial u_i}{\partial t} + \frac{\partial u_i \partial u_j}{\partial x_j} = -\frac{\partial p}{\partial x_i} + \nu \frac{\partial^2 u_i}{\partial x_j \partial x_j} + B u_i \tag{2}$$

and the conservation equation for a passive scalar:

$$\frac{\partial \theta}{\partial t} + \frac{\partial u_j \theta}{\partial x_j} = \alpha \frac{\partial^2 \theta}{\partial x_j \partial x_j} - \beta u_1 \tag{3}$$

where x_1, x_2 and x_3 are the coordinate axes ranging from 0 to 2π and u_i are the velocity components in those directions. The kinematic viscosity and diffusivity are indicated with ν and α, while Bu_i and $-\beta u_1$ are the forcing of the velocity field and the scalar

mean gradient (Rosales and Meneveau, 2005). The passive scalar field is monotonic (in the aforementioned sense), and, in the absence of diffusive effects, for $\alpha \to 0$, its governing equation in the Lagrangian form states that each particle transports the same (constant) value (Batchelor, 1959). It follows straightforwardly that it is conservative. Despite the linearity of conservation equation (3), a passive scalar introduced into a turbulent flow will very rapidly exhibit a wide variety of complex and chaotically evolving structures spanning all of the transporting velocity spectrum and more (Shraiman and Siggia, 2000).

The governing equations (1)-(3) are transformed in the spectral space, discretized on a uniform grid in a triply-periodic box and solved with a classic pseudo-spectral approach. The adopted time-advancement scheme is the semi-implicit fractional step method with a third order, explicit, memory-saving RK for the non-linear terms and an analytical integration of the (linear) viscous terms in the spectral space. All non-linear terms are treated with the 3/2 de-aliasing rule. Initial conditions are pseudo-randomly generated in the spectral space satisfying the divergence-free constraint and with a pre-assigned 3D spectrum (Mansour and Wray, 1994); the linear forcing guarantees that the stationary state is statistically independent of the artificially generated initial condition.

3. Loss of monotonicity of the passive scalar gradient

With a forced passive scalar field like the one in equation (3) scalar variance is produced by the forcing term and transported, without loss, throughout the inertial-convective range to the smallest scales where it is dissipated based on the balance:

$$\alpha\left(\frac{\partial\theta}{\partial x_j}\,\frac{\partial\theta}{\partial x_j}\right) = \beta\langle\theta u_1\rangle \tag{4}$$

where the statistical average operator $|\cdot|$ is substituted by the volume and time average operators invoking ergodicity of the flow. Throughout the cascade process many irregularities can occur. The purpose of the linear forcing is to constantly supply the cascade with a steady injection of scalar variance at the large-scales. In practical applications the variance is introduced in the flow by mean gradients, boundary conditions or source terms (for example, in reactive flows). In the absence of source terms the concentration equation is monotonic meaning that the maximum (minimum) value of the passive scalar concentration cannot increase (decrease) in time or space. However, the evolution equation for the gradient concentration looses its monotonicity even in the absence of source terms. Taking the gradient of equation (3) simply yields:

$$\frac{D}{Dt}\,g_i + \frac{\partial u_j}{\partial x_i}\,g_j = \alpha\frac{\partial^2 g_i}{\partial x_j \partial x_j} - \beta\frac{\partial u_1}{\partial x_i} \tag{5}$$

where the instantaneous scalar gradient is:

$$g_i = \frac{\partial\theta}{\partial x_i}. \tag{6}$$

The second term on the l.h.s. of equation (5) is the one responsible for the loss of monotonicity of the equation and it resembles the vortex stretching term. Its role can

be better understood by looking at the evolution equation for gradient norm $g = g_i g_i/2$ (or the instantaneous conservation equation of the scalar dissipation rate):

$$\frac{Dg}{Dt} = -g_i g_j \frac{\partial u_j}{\partial x_i} + \alpha \frac{\partial^2 g}{\partial x_j \partial x_j} - \alpha \frac{\partial g_i}{\partial x_j} \frac{\partial g_i}{\partial x_j} + \beta \frac{\partial u_1}{\partial x_i} g_i. \tag{7}$$

The first and third terms on the right-hand side are quadratic forms, therefore the anti-symmetric part of the tensors involved in them does not give contribution. Diffusion affects the scalar gradient in two ways: at small scales through the diffusion term $\partial^2(g_i g_i/2)/(\partial x_j \partial x_j)$, which may cause the gradient to locally increase or decrease, and with the instantaneous dissipation term $(\partial g_i/\partial x_j)^2$, which may only reduce the gradient. The term $-g_i g_j \partial u_j/\partial x_i$ is instead analogous to the vortex stretching term in the vorticity magnitude equation:

$$\frac{D}{Dt} \zeta = \zeta_i \zeta_j \frac{\partial u_j}{\partial x_i} + \nu \frac{\partial^2}{\partial x_j \partial x_j} \zeta - \nu \frac{\partial \zeta_i}{\partial x_j} \frac{\partial \zeta_i}{\partial x_j}. \tag{8}$$

where ζ_i is the ith vorticity component and $\zeta = \zeta_i \zeta_{i/2}$. This term is still present in the non-diffusive limit and the scalar gradient of a fluid particle can, therefore, evolve changing its module and direction in time. Following Raudkivi and Callander (1975) it can be shown that in the inviscid limit and without forcing, equation (7) becomes:

$$\frac{Dg}{Dt} = -g^2 \frac{\partial u_s}{\partial x_s} \tag{9}$$

where u_s and x_s are the velocity component and the curvilinear coordinate along scalar gradient lines, respectively. Therefore, even if the passive scalar energy must decay in time, energy associated to the scalar gradient could still sustain itself due to this term which could cause local discontinuities in the passive scalar gradient field, altering the structure of the passive scalar field itself leading to intermittency.

We suggest that such strong analogy between vorticity dynamics and the evolution of the scalar gradient field must be the starting point to shed some light on the source of the anomalous behavior of the passive scalar field. Taylor (1938) demonstrated, on average, that the vorticity was produced three times as fast as it was disappearing. One could argue that, analogously, the same happens to the scalar gradient, that hence sustains and increases itself in turbulence, independently of the presence of a forcing term. Future work will be directed towards this path and the purpose of following preliminary numerical is to acquire familiarity with the features of the scalar field reproducible with an incompressible flow model.

4. Numerical results

The results section is organized as follows. In Section 4.1 the time series of the scalar field and its gradients are shown, along with their PDFs. Then, In Section 4.2 the problems of the loss of isotropy, anomalous scaling and inertial sub-range intermittency will be addressed and the correspondent statistics presented. Finally, in Section 4.3, a brief interpretation of the anomalies will be given form a Lagrangian point of view. In all cases, averages have been carried out over a statistically steady time range of 80 large-eddy turnover times, τ. The simulation parameters are shown in Table I. We indicated with $Sc = v/\alpha$ the Schmidt number and with *CFL* the Courant number. Apart from the pressure term, the governing equations for the

scalar and the velocity field have been made identical in order to isolate the intrinsic differences of the two fields, those that do not depend on external factors such as forcing or initial conditions. Note that units for the simulation parameters such as the ones used in Table I are omitted since the reference time scales and length scales are arbitrary and are determined by the box size and the kinematic viscosity. What ultimately defines the state of turbulence is the Reynolds number based on the Taylor microscale and the Schmidt number. The parameters are similar to the ones adopted by Rosales and Meneveau (2005).

4.1 Time series and gradients

Strong non-Gaussian behaviors are present in time and space derivatives of θ and u_1, as shown by the exponential tails of PDFs in Figure 1. Intermittency effects are emphasized for the higher Reynolds number cases as expected. PDFs of θ and u_1, however, do not exhibit a well-defined non-Gaussian shape (not shown). The time series of spatial and temporal derivatives at one point (scaled by τ – Figures 2 and 3(a) and (b)) exhibit aperiodic large jumps which stand out with respect to the rest of the signal. On the other hand, these features are not evident in the time series of the scalar field itself, although low-frequency modes resembling the "cliff structures" (Wahraft, 2000) are still rather evident (Figure 4(a) and (b)). This supports the premise of our analytical considerations in Section 3 that non-Gaussian behaviors in the gradient field are due to the second term on the left-hand side of equation (5), not present in equation (3).

Strong non-Gaussian behaviors have also been found in the PDFs of the time derivatives (Figure 5). The abrupt changes in the time series of the derivatives, which arise at small scales, are consistent with the unboundedness of g(9). These peaks can be modeled as Dirac functions, which modify the statistical structure of the gradients, broadening the sample space and the spectrum, therefore leading to the presence of exponential tails in the correspondent PDFs. While the connection between the

N^3	L	v	Sc	B	β	CFL
96^3	2π	2.8×10^{-3}	1	0.1333	-0.1333	0.3
128^3	2π	1.272×10^{-2}	1	1	-1	0.3

Table I.
DNS parameters

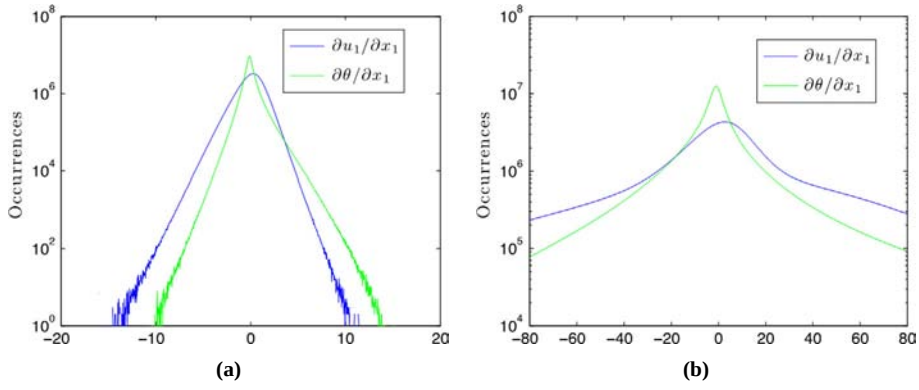

Figure 1.
PDFs of derivatives of u_1 (blue) and θ (green) along x_1 for $N^3 = 96^3$ (a) and $N^3 = 128^3$ (b)

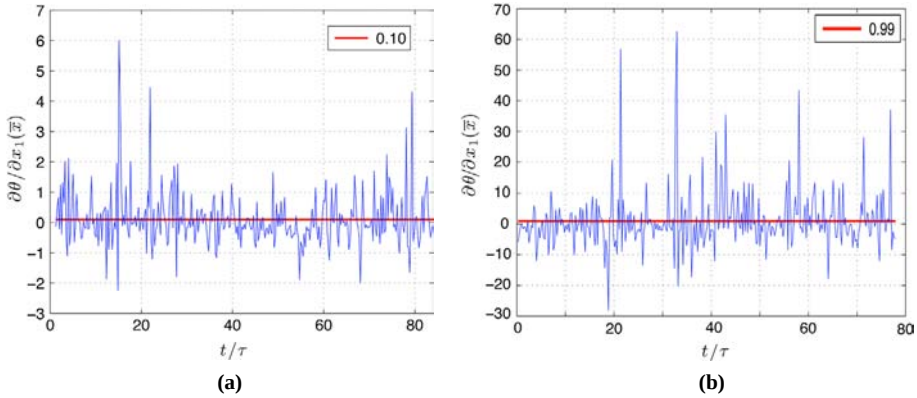

Figure 2.
Time series of $\partial\theta/\partial x_1$ for $N^3 = 96^3$ (a) and $N^3 = 128^3$ (b) extracted at one point with time-average (red line)

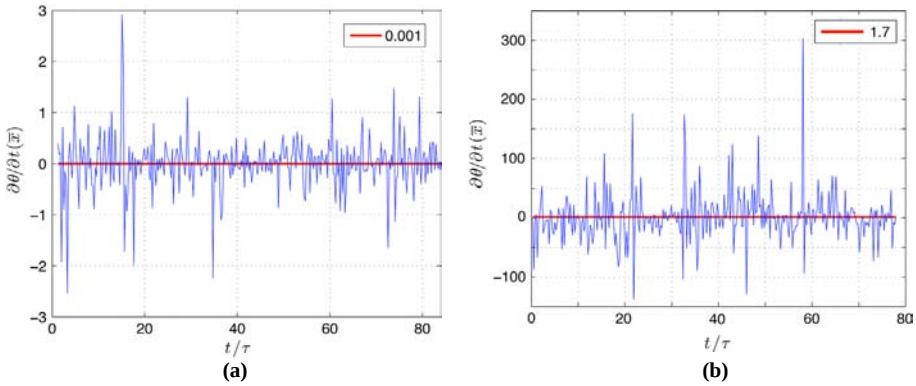

Figure 3.
Time series of $\partial\theta/\partial t$ for $N^3 = 96^3$ (a) and $N^3 = 128^3$ (b)

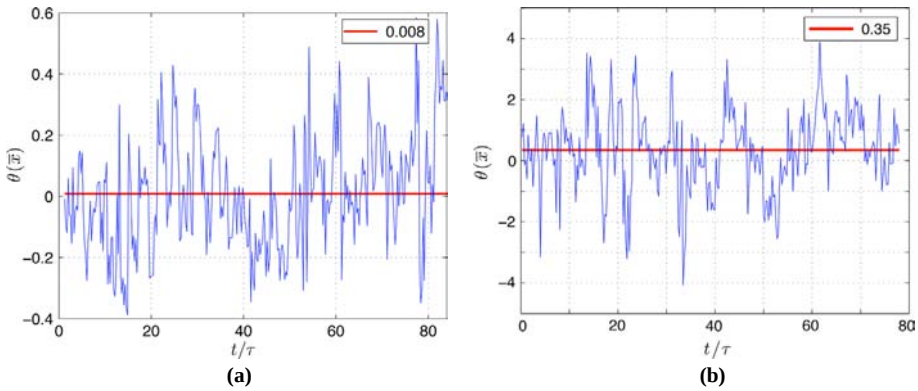

Figure 4.
Time series of θ for $N^3 = 96^3$ (a) and $N^3 = 128^3$ (b)

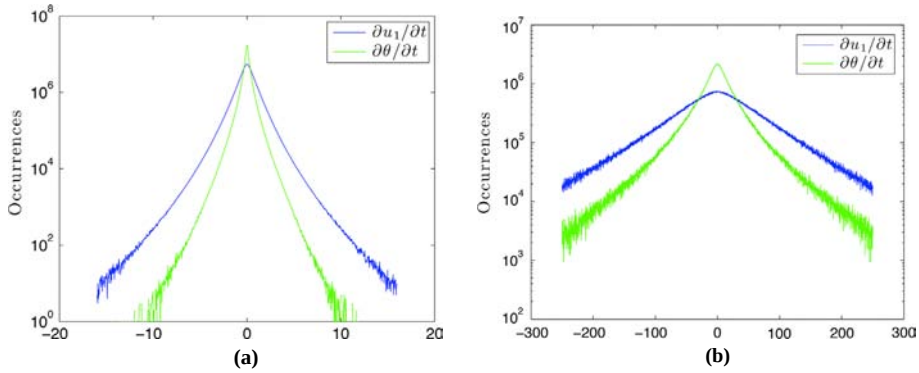

Figure 5.
PDFs of time derivatives of u_1 (blue) and θ (green) for $N^3 = 96^3$ (a) and $N^3 = 128^3$ (b)

non-Gaussian behaviors and the presence of the first term on the right-hand side of equation (7) is explained by the violent burst created by the latter in the gradient time series, the connection with the ramp-cliff structures is less straightforward. The loss of isotropy is typically explained by a coupling between small scales (violent burst in the gradients) and large-scales (ramp-cliff structures in the scalar time series). The presence of a mean gradient emphasizes the anomalies in odd-moments that would be otherwise hidden by symmetries (Wahraft, 2000). It therefore seems that imposing a mean gradient (first odd-moment) "unlocks" all the other moments. The sharper are the cliffs, the more intermittent are the gradients, while the Skewness (third order moment, discussed later) remains essentially the same. All these behaviors can be verified in our results; nevertheless, this global picture provides only an indirect way to connect ramp-cliffs and gradients (gradients create intermittence via the violent bursts, while sharper cliffs, created by spikes in the gradient time series, enhance it). We believe, however, that the two scale effects are not independent. Violent bursts are present only in time- and space-derivatives time series (Figures 2 and 3), while ramp-cliffs are only present in the scalar time series (Figure 4). Being the scalar field the time-integral of its derivatives and modeling its violent burst as impulses, we can interpret the ramp-cliffs (large-scale) structures, mathematically, as resulting from the integration of these (small scale) impulses, which are known to lead to (large scale) steps mathematically. The aforementioned direct influence between large- and small-scales is present both in time (ramp-cliffs) and space (large fronts, discussed later), as both spatial and temporal directions are statistically equivalent in our case (homogenous and statistically stationary field). The connection between the effect of the loss of moniticity in the gradient equation (9), intermittency (due to the resulting violent burst) and the ramp-cliffs structures is now evident, and consistent with the mathematical framework provided.

Due to the presence of the mean gradient, PDFs of spatial derivatives along x_1 direction (Figure 1) are not symmetric, therefore positive and negatives values are not equiprobable. Statistics of the spatial derivatives along directions x_2 and x_3 (not shown here) present in fact the same non-Gaussian behavior seen for the x_1 direction, with the only difference that no asymmetries are observed. These statistics can be compared with those for the vorticity field (not shown here), well described in the literature, such as in the work by Jiménez *et al.* (1993) for low and high Reynolds numbers and, more recently, by Wilczek and Friedrich (2009), where intermittency was observed to increase with

the Reynolds number. The similarities with the statistics of the scalar field are striking, although a more marked intermittent behavior is exhibited in the latter.

Non-Gaussian behaviors have been also observed in second-order statistics. In Figure 6 the correlation $\theta\varepsilon_\theta$ where ε_θ is the scalar dissipation function, is shown. Again, intermittency effects seem to increase with the Reynolds number also in this case.

4.2 Loss of isotropy, anomalous scaling and inertial intermittency

Intermittency effects extend also in the inertial sub-range, despite the rather low Reynolds numbers investigated here. They are evident in the PDF of the scalar differences (Figure 7). At small scales non-Gaussian behaviors are prevalent, and there is a fast tendency towards Gaussianity at larger scales. This result is consistent with the calculated scalar intermittency exponents for these cases. The intermittency exponent μ_θ was computed by comparing the scalar dissipation autocorrelation function:

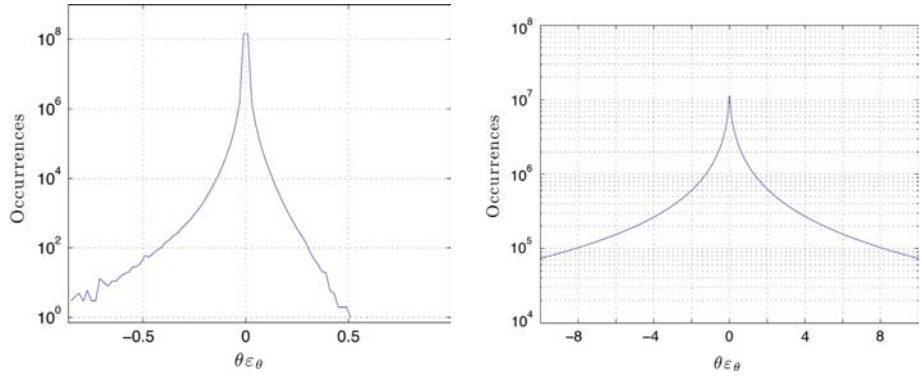

Figure 6.
PDFs of $\theta_{\varepsilon\theta}$ for $N^3 = 96^3$ (a) and $N^3 = 128^3$ (b)

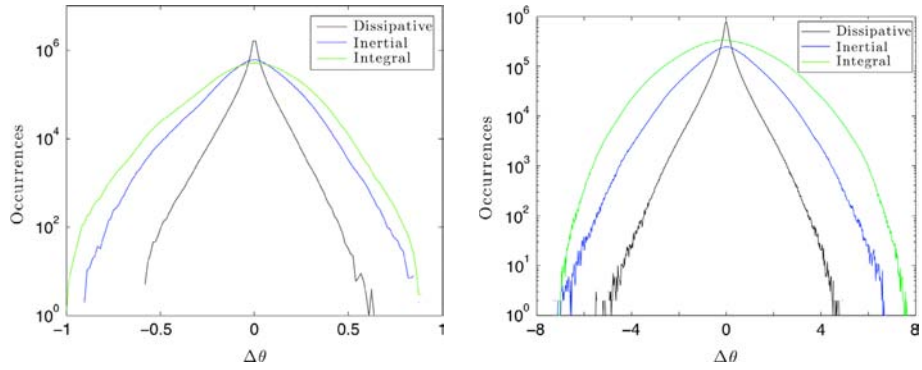

Figure 7.
Function $\Delta\theta(r)$ at small, medium and integral scales

Notes: Inertial scale has been estimated in the range $25\eta < r < 35\eta$ for the $N^3 = 96^3$ case (a) and $28\eta < r < 40\eta$ for the $N^3 = 128^3$ case (b); small and integral range have been estimated, respectively, in the ranges $0 < r < 10\eta$ and $l_0 < r < 1.5l_0$ for both the simulations (η and l_0 differ between the two simulations)

$$\rho_{\in\theta} = \frac{< \varepsilon_\theta(x)\varepsilon_\theta(x+r) >}{< \varepsilon_\theta^2 >}$$

with:

$$\rho_{\in\theta} = ar^{-\mu s} + b$$

where a and b are calculated by least-square fit for a given μ_θ. In Figure 8(a) the two trends for the $N^3 = 96^3$ simulation are presented. There is fair agreement between the two curves for small and medium separations in space, where intermittency effects are expected to be more evident. In particular, an intermittency exponent $\mu_\theta = 0.1$ has been found at $\mathrm{Re}_\lambda = 50$ with coefficients $a = 0.14$ and $b = 1.32$. The same results hold for the higher Reynolds number case (not shown). This value is slightly below the one found in literature, which refers to a higher Reynolds number ($90 < \mathrm{Re}_\lambda < 700$). Intermittency effects are expected to be weaker in the range of Reynolds numbers covered in the present work.

Loss of isotropy at small scales is also evident. Statistics at small scales depend on the particular direction, visible through third and fourth order statistics. For a real random quantity q, the skewness is a measure of the asymmetry of the probability distribution of q, while the kurtosis is a measure of its "peakedness". In the case of two points correlations in turbulence, both are function of the separation r. The KOC theory suggests that the passive scalar derivative skewness is of order one along the mean gradient direction and of order Re_λ^{-1} along the orthogonal directions. Consistently, the scalar derivative skewness is 1.5 in the $N^3 = 96^3$ simulation, and 1.4 in the $N^3 = 128^3$ simulation (Figure 9). No Reynolds number effects are observed.

Time-averaging over 80 τ reveals persistent "hot-cold" fronts in the instantaneous fields (Figure 10). These are the equivalent in space of the localized bursts occurring in the time series. A front in the scalar field can be seen as the integral of an impulsive (Dirac function), strong intermittent gradient in the space; analogously, a ramp-cliff structure is seen as the result of the integral of strong peaks in the scalar gradient in time.

This behaviour is not immediately understood but small-scale statistics can provide useful insight, since the time series burst are a small-scale feature. Loss of symmetry is evident in the skewness of the scalar difference, $S\Delta\theta$, which depends on

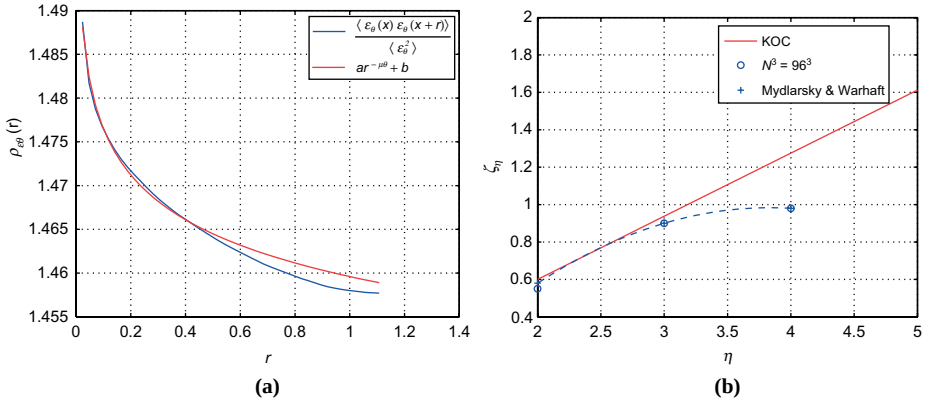

Figure 8.
Autocorrelation function of the scalar dissipation $\rho_{c\theta}$ (a); scaling exponents interpolation as function of the structure function order n (b)

the direction at small scales (Figure 11). SΔθ flattens out in the inertial sub-range before approaching the smallest scales. However, we notice that plateau is present at the smallest scales only along the gradient direction (direction x_1) and behave differently along the others. This last result, together with the tendency of the scalar difference kurtosis towards the Gaussian value of 3 only at large-scales (Figure 12) is consistent with the well-known scalar "anomalous scaling". Moreover, the scaling exponents ζ_n in function of the order n (Figure 8(b)) are in perfect agreement with results in Figure 11 of Wahraft (2000).

While the Kolmogorov's constant for the spectrum is fairly well established as CK = 1.3974 (for very high Reynolds numbers), there is still no agreement on the value of the Obukhov-Corrsin constant. Our findings show an optimal value for $C\theta = 0.80$, higher than that found by Mydlarsky and Warhaft (1998), which is in the range 0.54-0.55. The reason lies in the much higher Reynolds numbers achieved experimentally by Mydlarski and co-workers. In Figure 12(b) it is possible to see how the energy spectra for the

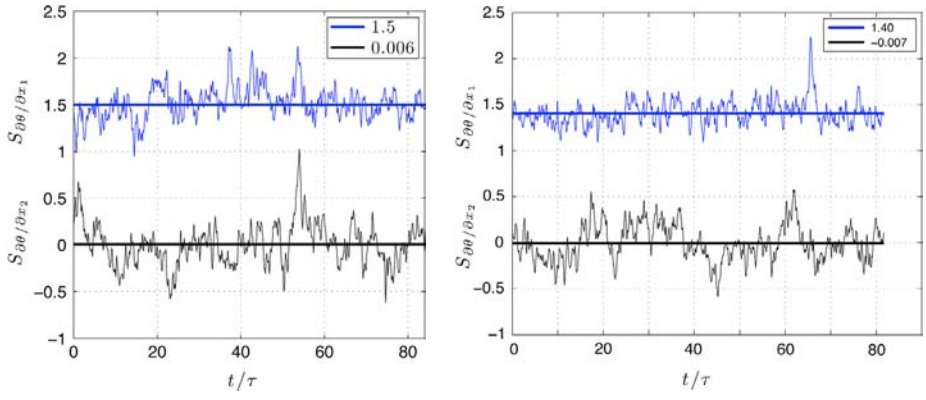

Figure 9.
Passive scalar derivative skewness in the x_1 (blue) and x_2 (black) direction for $N^3 = 96^3$ (a) and $N^3 = 128^3$ (b)

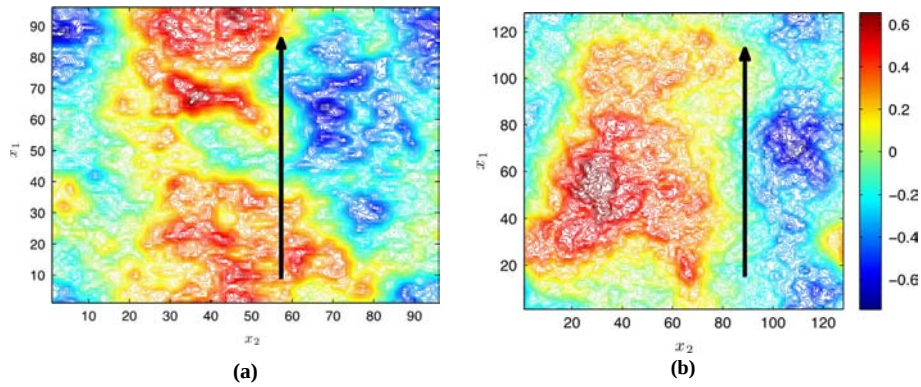

Figure 10.
Fronts occurring in plane $x_1 - x_2$ of the statistically averaged passive scalar field for $N^3 = 96^3$ (a) and $N^3 = 128^3$ (b)

Note: Arrows shows direction of the "hot-cold" fronts, which is also the scalar mean gradient direction

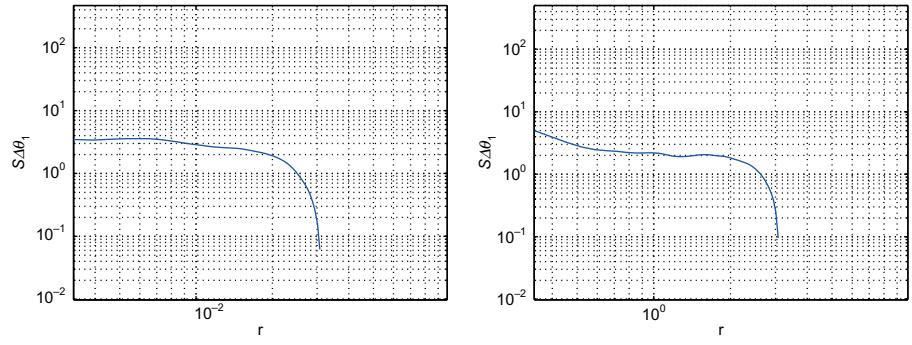

(a) Direction x_1 **(b)** Direction x_2

Figure 11.
Scalar difference skewness $S_{\Delta\theta}$ along directions x_1 (a) and x_2 (b)

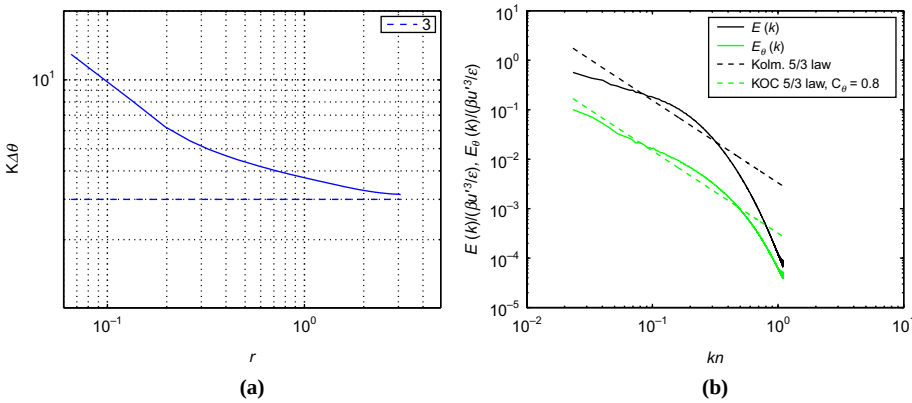

(a) **(b)**

Figure 12.
Passive scalar differences kurtosis as a function of $r(a)$ and kinetic energy and scalar variance spectra compared with the Kolmogorov's and KOC's $-5/3$ spectra (b)

velocity and passive scalar fields reported agree quite well the $-5/3$ laws. The case at $N^3 = 128^3$ (not shown) produces essentially the same results.

4.3 Lagrangian paths

A Lagrangian analysis is carried out here to compare our predictions with the theories of Taylor for the diffusion of a single particle and Richardson for the diffusion of two particles (Davidson, 2004). This approach has been chosen since it is considered effective to shed light on fundamental questions in fluid mechanics and, in particular, to "capture the intrinsic nature of turbulence" which, as stressed in Sreenivasan and Shumacher (2010), lies in Lagrangian flow dynamics.

The passive scalar field, in the absence of source terms, preserves its value along a trajectory, i.e. from a Lagrangian perspective (Section 3). However, in turbulence we must consider the statistical average, given in this case by the Langevin ensemble at point t and position r (Shraiman and Siggia, 2000). The mean value of $\theta(r,t)$ can be derived projecting all trajectories onto the Green's function which, representing the probability of a trajectory to arrive at point t and position r by starting from t' and r',

takes on the form of a Lagrangian PDF. Since the (average) trajectory of a particle does not depend on its initial position (due to homogeneity), one point and one-time PDFs in Eulerian and Lagrangian forms are identical, and Eulerian quantities can therefore be derived from a Lagrangian PDF model. Moreover, after a certain time, the particle looses the "memory" of its source, i.e. the value of Green's function in the integral becomes low, since it can roughly be regarded as the integral in time of the Lagrangian autocorrelation coefficient. Mixing times on each trajectory, however, depend on the particular velocity realization, and statistical averaging is still possible. Because of this, large excursion of θ can occur even when mixing is weak, leading to the exponential tails. In our particular case, the gradient is amplified along the path by the strain, but this amplification is still controlled by the trajectory average, and therefore the same conclusions can be drawn (Shraiman and Siggia, 2000).

In this work the paths of 50 particles have been analyzed with starting positions inside a sphere of a radius corresponding to half the Kolmogorov length scale. The plots in Figure 13 refer to the case for $N^3 = 96^3$. The solid red lines represent the predictions of the Taylor theory at small scales in Figure 13(a) and the Richardson theory in the inertial subrange in Figure 13(b), while the green lines represent the same predictions at larger scales. The agreement between our results and the theory is not as satisfactory in the dissipation-range and, in particular, for the relative diffusion of two particles (Figure 13(b)). Richardson's law for the inertial range predicts a scaling of $R \sim t^{3/2}$ which well matches our results (with a Richardson's constant found

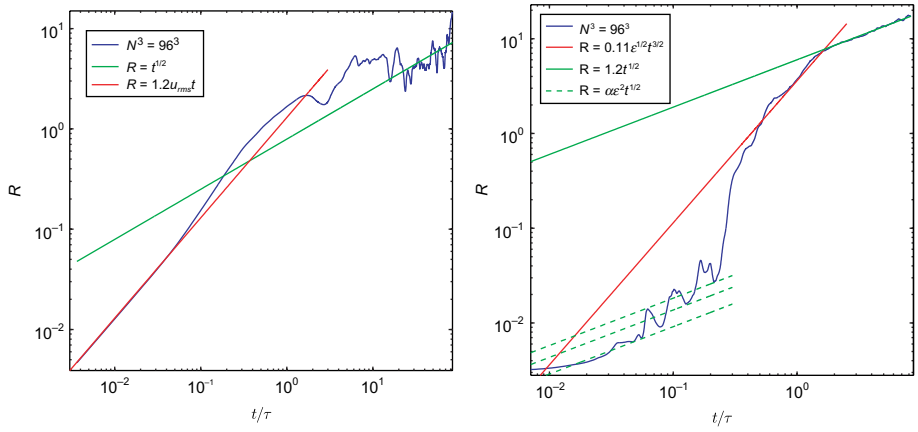

Figure 13.
Averaged distance (a) and relative distances (b) covered by 50 particles from their starting position for the simulations $N^3 = 96^3$ confronted, respectively, with Taylor and Richardson theories

Notes: In Figure (a) the red line represents the small-scales Taylor predictions ($R \sim t$) while the green line represents the large-scale Taylor predictions ($R \sim t^{1/2}$); in Figure (b) the red line represents instead the inertial-range Richardson's law ($R \sim t^{3/2}$) and the green (continuous) line the large-scale scaling ($R \sim t^{1/2}$); dotted lines represent small scales scaling $R \sim t^{1/2}$ based on large-small-scale analogy approach; values of coefficient a are $a = 1$, $a = 1.5$ and $a = 2$; Kolmogorov scale is $\eta = 0.023 = \varphi\,(10^{-22})$ in the logarithmic plot; curves are scaled with the mean dissipation-rate powers to obtain order-one coefficients; notice how this does not imply that all coefficients are non-dimensional

to be ≈ 0.11, red line). At large-scales, a better scaling $R \sim t^{1/2}$ must be preferred to Richardson's law (Davidson, 2004). Based on the general idea that turbulence does not affect significantly the particles' path at small scales (because of viscosity) and at large-scales, it could be suggested to adopt the same scaling $R \sim t^{1/2}$ at small scales. However, this scaling appears inadequate (dot lines). A better agreement could be obtained by changing the exponent for t from 1/2 to a value between 1/2 and 3/2, or switching to a more-than-linear behavior (in the log-log plot). This is consistent with the behavior of the power spectra (derived from an Eulerian approach) in the dissipation-range, where the behavior deviates from the Kolmogorov's $-5/3$ power law (consequence of self-similarity) to a more-than-linear decay (in the log-log plot). In fact the energy (Eulerian) spectrum (Figure 12(b)) decays at small scale with a more-than-linear law (in the log-log plot). This analogy is not casual and it highlights the connection between the Eulerian and the Lagrangian phenomenology. We speculate that the nature of the disagreement at small scales in Figure 13(b) is a result of the typical loss of self-similarity in the passive scalar in the dissipation-range.

Another property that can be observed is the following. The mean relative-distance transitions from a dissipation-range behavior to an inertial-scale behavior quite rapidly at approximately 2.2/2.3 turnover times, when the relative distance is around 1.3/1.4 times the Kolmogorov's scale ($\eta = 0.023$ in the $N^3 = 96^3$ simulation). This sudden transition is consistent with the literature (Davidson, 2004).

Finally, In Figure 13(a) results from the Taylor theory are compared with ours. We observe a small increase of slope respect to the Taylor small-scale predictions ($R_{\sim t}$) at about 0.04 turnover times. This corresponds to when a particle has moved, on average, along a distance of about 2.3 η. This change is due to the fact that the particle separation is entering the inertial range.

In spite of the self-consistency of the results presented, more accurate simulations and at higher Reynolds are needed to assess the speculations made. High Reynolds numbers lead in fact to an increase of intermittency effects (Wahraft, 2000), therefore emphasizing the anomalous behavior of the passive scalar in a turbulent flow.

5. Conclusions

We have performed a study on intermittency effects with DNS of a unitary-Schmidt-number scalar in a turbulent flow for $\mathrm{Re}_\lambda = 50$ and $\mathrm{Re}_\lambda = 70$. Classic results regarding inertial-range intermittency are reproduced such as non-Gaussian behavior of passive scalar statistics, loss of local isotropy, multi-fractal scaling of scalar structure functions. A new approach is proposed here based on the interpretation of intermittency in terms of loss of regularity, at smallest scales, of the evolution equation of the scalar gradient. In spite of the low Reynolds numbers investigated non-Gaussianity was still very evident, especially in the PDFs of the scalar gradient, while the scalar and the velocity PDFs remain perfectly Gaussian. This is consistent with the main conclusion of the paper that sources of anomalies in the scalar field derive from the loss of mathematical constraints on the boundedness of the scalar gradient field. The time series of the gradients exhibit large jumps that acting as Dirac functions may lead to the observed exponential tails in the respective distribution. We speculate that this mechanism is also responsible for the loss of universality of the passive scalar field at the small scales, observed in particular in the Lagrangian analysis whose results are compared with the diffusion theory of two particles.

We suggest, in conclusion, that future investigation on the topics of intermittency and anomalies in the passive scalar field should start from the mathematical analysis of the boundedness properties of the scalar gradient transport equation, carried out, if possible, from a Lagrangian perspective.

References

Antonia, R.A. and Orlandi, P. (2003), "Effect of schmidt number on small-scale passive scalar turbulence", *Appl. Mech. Rev.*, Vol. 56 No. 6, pp. 615-32.

Antonia, R.A., Chambers, A.J., Britz, D. and Browne, L.W.B. (1986), "Organized structures in a turbulent plane jet: topology and contribution to momentum and heat transport", *J. Fluid Mech.*, Vol. 172, pp. 211-29.

Batchelor, G.K. (1959), "Small-scale variation of convected quantities like temperature in turbulent fluid Part 1. General discussion and the case of small conductivity", *J. Fluid Mech.*, Vol. 5 No. 1, pp. 113-33.

Chen, S. and Kraichnan, R.H. (1998), "Simulations of a randomly advected passive scalar field", *Phys. Fluids*, Vol. 10 No. 11.

Davidson, P. (2004), *Turbulence: An Introduction for Scientists and Engineers*, Oxford University Press, New York, NY.

Frisch, U. (1995), *Turbulence: the Legacy of A.N. Kolmogorov*, Cambridge University Press, Cambridge.

Holzer, M. and Siggia, E.D. (1994), "Turbulent mixing of a passive scalar", *Phys. Fluids*, Vol. 6 No. 5.

Jiménez, J., Wray, A.A., Saffman, P.G. and Rogallo, R.S. (1993), "The structure of intense vorticity in isotropic turbulence", *J. Fluid Mech.*, Vol. 255, pp. 65-90.

Kolmogorov, A.N. (1941), "Dissipation of energy in the locally isotropic turbulence", *Proceedings: Mathematical and Physical Sciences*, Vol. 434, pp. 15-17.

Kraichnan, R.H. (1994), "Anomalous scaling of a randomly advected passive scalar", *Phys. Rev. Lett.*, Vol. 72 No. 7, pp. 1016-19.

Leveque, R.J. (2002), *Finite Volume Methods for Hyperbolic Problems*, Cambridge University Press, Cambridge.

Mansour, N.N. and Wray, A.A. (1994), "Decay of isotropic turbulence at low Reynolds number", *Phys. Fluids*, Vol. 6 No. 2, pp. 808-14.

Meneveau, C. and Sreenivasan, K.R. (1990), "Interface dimension in intermittent turbulence", *Phys. Rev. A*, Vol. 41 No. 4, pp. 2246-8.

Mydlarsky, L. and Warhaft, Z. (1998), "Passive scalar statistics in high-Peclet-number grid turbulence", *J. Fluid. Mech.*, Vol. 358 No. 1, pp. 135-75.

Obukhov, A.M. (1949), "Structure of the temperature field in turbulent flows", *Izv. Akad. Nauk SSSR, Ser. Geogr. Geofiz.*, Vol. 13 No. 1, pp. 58-69.

Pope, S.B. (2000), *Turbulent Flows*, Cambridge University Press, Cambridge.

Raudkivi, A.J. and Callander, R.A. (1975), *Advanced Fluid Mechanics: An Introduction*, Wiley, New York, NY.

Rosales, C. and Meneveau, C. (2005), "Linear forcing in numerical simulations of isotropic turbulence: physical space implementations and convergence properties", *Phys. Fluids*, Vol. 17 No. 9, pp. 095106-095106-8.

Ruiz-Chavarria, G., Baudet, C. and Ciliberto, S. (1996), "Scaling laws and dissipation scale of a passive scalar in fully developed turbulence", *Physica D*, Vol. 99 Nos 2/3, pp. 369-80.

Shraiman, B.I. and Siggia, E.D. (2000), "Scalar turbulence", *Nature*, Vol. 405 No. 8, pp. 639-46.

Sreenivasan, K.R. and Shumacher, J. (2010), "Lagrangian views on turbulent mixing of passive scalars", *The Royal Society*, Vol. 368 No. 1916, pp. 1561-77.

Sreenivasan, R. (1991), "On local isotropy of passive scalars in turbulent shear flows", *Mathematical and Physical Sciences*, Vol. 434, pp. 165-82.

Taylor, G.I. (1938), "Production and dissipation of vorticity in a turbulent fluid", *Proc. R. Soc. Lond. A*, Vol. 164, pp. 15-23.

Vedula, P., Yeung, P.K. and Fox, R.O. (2001), "Dynamics of scalar dissipation in isotropic turbulence: a numerical and modelling study", *J. Fluid Mech.*, Vol. 433 No. 1, pp. 29-60.

Wahraft, Z. (2000), "Passive scalars in turbulent flows", *Annu. Rev. Fluid Mechanics*, Vol. 32, pp. 203-40.

Wilczek, M. and Friedrich, R. (2009), "Dynamical origins for non-Gaussian vorticity distribution in turbulent flows", *Phys. Rev. E*, Vol. 80 No. 1, pp. 6316-22.

Corresponding author
Ivan Langella can be contacted at: ivanlang87@gmail.com